Zoology 117 (2014) 269–281

Contents lists available at ScienceDirect

Zoology

journal homepage: www.elsevier.com/locate/zool

Center of mass motion in swimming fish: effects of speed and locomotor mode during undulatory propulsion

Grace Xiong, George V. Lauder*

Museum of Comparative Zoology, Harvard University, 26 Oxford Street, Cambridge, MA 02138, USA

ARTICLE INFO

Article history:
Received 18 December 2013
Received in revised form 27 February 2014
Accepted 3 March 2014
Available online 12 May 2014

Keywords:
Fish locomotion
Swimming kinematics
Center of mass motion

ABSTRACT

Studies of center of mass (COM) motion are fundamental to understanding the dynamics of animal movement, and have been carried out extensively for terrestrial and aerial locomotion. But despite a large amount of literature describing different body movement patterns in fishes, analyses of how the center of mass moves during undulatory propulsion are not available. These data would be valuable for understanding the dynamics of different body movement patterns and the effect of differing body shapes on locomotor force production. In the present study, we analyzed the magnitude and frequency components of COM motion in three dimensions (*x*: surge, *y*: sway, *z*: heave) in three fish species (eel, bluegill sunfish, and clown knifefish) swimming with four locomotor modes at three speeds using high-speed video, and used an image cross-correlation technique to estimate COM motion, thus enabling untethered and unrestrained locomotion. Anguilliform swimming by eels shows reduced COM surge oscillation magnitude relative to carangiform swimming, but not compared to knifefish using a gymnotiform locomotor style. Labriform swimming (bluegill at 0.5 body lengths/s) displays reduced COM sway oscillation relative to swimming in a carangiform style at higher speeds. Oscillation frequency of the COM in the surge direction occurs at twice the tail beat frequency for carangiform and anguilliform swimming, but at the same frequency as the tail beat for gymnotiform locomotion in clown knifefish. Scaling analysis of COM heave oscillation for terrestrial locomotion suggests that COM heave motion scales with positive allometry, and that fish have relatively low COM oscillations for their body size.

1. Introduction

As a representation of the total forces exerted on an animal, center of mass (COM) movement provides important information on locomotor dynamics and can be used to calculate energy expenditure, efficiency, and the effect of ground reaction forces on limbs (Biewener, 1989; Ortega and Farley, 2005). In horses, humans, and other terrestrial animals, COM movement is used to compare work done over different gaits (Blickhan and Full, 1987; Pfau et al., 2006; Kuo, 2007; Biknevicius et al., 2013). It is also used to describe the effect of limbs on whole body movements, especially where the limbs comprise a significant portion of the body's mass (Abourachid et al., 2011; Walter and Carrier, 2011). COM oscillation patterns are even used as a "locomotor signature" to identify pathological gaits or evolutionary trends (e.g., Clemente et al., 2008; Minetti et al., 2011).

Despite the breadth of research that has been done on terrestrial and aerial COM movement during animal locomotion and its importance in understanding animal dynamics, almost nothing is known about COM movement in fishes during undulatory locomotion. This is especially surprising given the extensive descriptive literature defining and comparing body kinematic patterns in fishes, with the accompanying proliferation of terminology to describe body motions. Anguilliform (eel-like), carangiform (jack-like), labriform (wrasse-like), and gymnotiform (knifefish-like) are just a few of the terms used to describe fish swimming patterns (Webb, 1975; Sfakiotakis et al., 1999; Shadwick and Lauder, 2006). These terms are meant to reflect broad kinematic differences among fish species and generally how thrust is generated during locomotion by the body and fins. But how differing body movement patterns affect COM motion remains unknown, and the effects of changing swimming speed on COM oscillation amplitude in fishes with different body shapes are likewise not yet understood. Due to differences in locomotor media and in the use of limbs on land compared to thrust generation using body deformation in the water, amplitudes and frequencies of COM oscillation could differ substantially between aquatic and terrestrial animals.

The limited data from steadily rectilinearly swimming fishes in which COM oscillations have been experimentally measured includes quantification of COM motion data during pectoral fin

* Corresponding author. Tel.: +1 617 496 7199.
E-mail address: glauder@oeb.harvard.edu (G.V. Lauder).

http://dx.doi.org/10.1016/j.zool.2014.03.002
0944-2006/

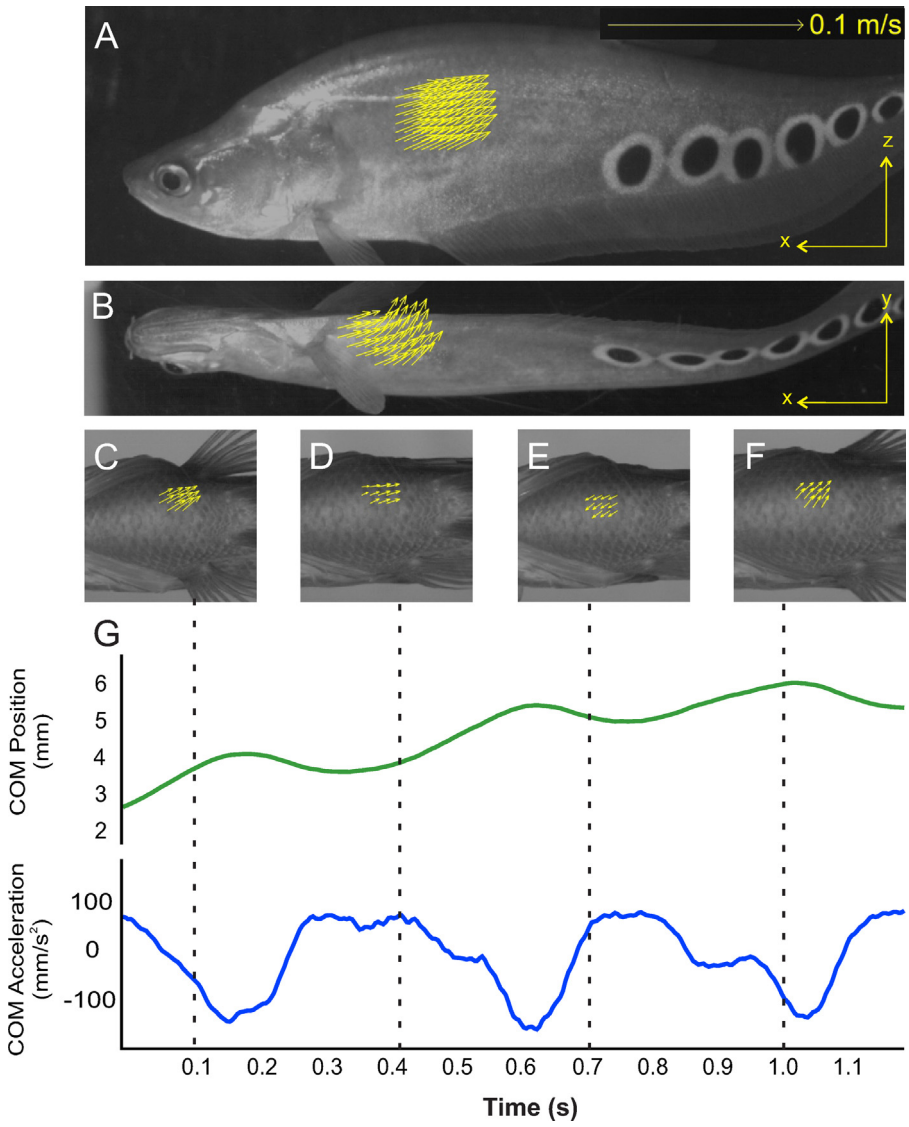

Fig. 1. Method of center of mass (COM) analysis using particle image velocimetry cross-correlation. Fish were filmed while holding as steady a position as possible during swimming at speeds of 0.5, 1.0, and 1.5 BL/s. A velocity vector field was created over the area of the COM in both lateral (A) and ventral (B) views, shown for *Notopterus chitala* in these two panels. Sample variation through time (C–F) is shown in ventral view for *Lepomis macrochirus*, and COM velocity can be seen moving backward and then forward in panels (C), (D), and (E). Dashed lines mark the time positions of panels (C)–(F) on the graphs below. Velocity vectors were averaged to give a mean velocity through time, which was then integrated for the displacement, and the derivative taken for acceleration (G). This fish (*L. macrochirus*) drifted several mm downstream during this sequence, and hence there is a slight trend in COM position that was removed by regression analysis (see Sections 2.3 and 2.4 for more information on how the COM data were analyzed). A supplementary online movie in the Appendix shows velocity vectors over the center of mass in a swimming bluegill sunfish.

locomotion (Walker and Westneat, 1997; Walker, 2004; Lauder and Madden, 2008) and an analysis by Tytell (2007) who estimated COM velocity in two swimming fish species by digitizing the position of the tip of the snout. Other than these investigations, we are not aware of any measurements of COM motion in steadily swimming fishes.

The overall goal of the present paper is to analyze in three dimensions the COM motion of several fish species (eel, bluegill sunfish, and clown knifefish) swimming with four locomotor modes at three speeds. We used high-speed video and an image cross-correlation technique to enable untethered and unrestrained locomotion, so that COM motion is not influenced by attachment of transducers or any drag forces that might result from transducer wires. Specifically, we quantified COM velocities in three dimensions (x: surge; y: sway, and z: heave) and then calculated COM displacement and acceleration from the velocity data. We tested for differences among species swimming with different locomotor modes, and also wanted to see how changes in swimming speed alter COM motion during undulatory swimming. Hypotheses examined include the following: (i) anguilliform locomotion will show reduced surge COM oscillations compared to carangiform swimming; (ii) labriform locomotion will show reduced sway COM oscillations but increased surge oscillations compared to other undulatory modes; (iii) the gymnotiform combination of simultaneous body and fin motion will permit reduced COM oscillations in both the surge and sway directions; and (iv) surge COM oscillations will occur at either two or four times the tail beat frequency based on the data presented in Tytell (2007).

2. Materials and methods

2.1. Study animals

Four clown knifefish (*Notopterus chitala*, Hamilton, 1822) measuring 19.1 ± 0.5 cm (mean ± standard error) in total length with masses of 44.9 ± 1.5 g and body surface area of 69.8 ± 1.6 cm^2 were

acquired from a local pet store and kept in 40 l tanks at 25 °C. Three bluegill sunfish (*Lepomis macrochirus*, Rafinesque, 1819) measuring 20.4 ± 0.3 cm with masses of 149.9 ± 10.9 g and body surface area of 104.3 ± 9.8 cm^2 were collected locally under our scientific collection permit (Massachusetts, USA) and kept in individual 40 l tanks at 18 °C. Three American eels (*Anguilla rostrata*, Lesueur, 1817) measuring 31.0 ± 1.8 cm with masses of 35.6 ± 5.7 g and surface area of 48.7 ± 5.1 cm^2 were also collected locally and kept in individual 30 l tanks at 18 °C.

These three species were chosen a priori to reflect different locomotor styles and to represent a diversity of modes of swimming in fishes. Bluegill sunfish have a deep and narrow-width body, and use a labriform locomotor mode where thrust forces are generated exclusively by the pectoral fins at swimming speeds of less than about 1.0 body lengths (BL)/s (Gibb et al., 1994; Drucker and Lauder, 1999). At higher speeds bluegill use a carangiform or "subcarangiform" swimming mode in which thrust is generated primarily by body oscillations. This species is thus a good experimental subject for this study as it undergoes a prominent gait transition between the lowest and the two highest swimming speeds tested here. Eels exemplify the anguilliform swimming mode with smaller wavelength body waves that increase in amplitude down the body. Only at speeds higher than those tested here do body waves begin to generate larger lateral oscillations of the anterior half of the fish. The narrow and elongate eel shape contrasts with the deep body of bluegill sunfish. Knifefish display the gymnotiform locomotor mode in which body undulations combined with undulation of the elongated ventral anal fin are used to power swimming. The elongated anal fin is actuated by fin muscles that are independent of the myotomal body muscles that produce body waves during locomotion, and anal fin and body waveforms are thus somewhat decoupled from each other in swimming clown knifefish.

2.2. Anatomical COM measurement

The anatomical COM of bluegill sunfish (*L. macrochirus*) has been measured in previous studies (Drucker and Lauder, 1999, 2001; Tytell and Lauder, 2008). For *A. rostrata* and *N. chitala*, two specimens each from the Museum of Comparative Zoology (Cambridge, MA, USA) of similar body size to the live specimens studied here were used to calculate COM position. The fish were stiff and straight from preservation and were hung from three points on the body with strings and allowed to come to a rest before being photographed. The photographs were overlaid and the intersection of the strings was taken as the COM.

The anatomical COM position of *L. macrochirus* lies at 40% of total body length (including the caudal fin) from the tip of the nose and 50% of the body width, excluding the dorsal fin (Drucker and Lauder, 2001; Tytell and Lauder, 2008). The mean COM position of *A. rostrata* lies at 46% of the body length from the tip of the nose. Mean COM position of *N. chitala* was at 25% of the body length from the tip of the nose, and just over halfway up the height of the fish.

Since the center of mass marks the midpoint of body mass in three-dimensional (3D) space, the COM moves over the course of a tail beat cycle as the body bends: if the fish body is strongly bent, the COM can be positioned outside the body. For the locomotor modes studied here, the extent of unidirectional body bending is small, the portions of the body that are bending contain little mass relative to the anterior region of the body and head, and wave-like body bending results in only a small change in lateral mass distribution since wave-like motion deflects body mass to both sides of the COM. A previous study (Tytell and Lauder, 2008) tracking the true COM position during a C-start escape response showed only very small variation in COM position even when the tail was bent at almost 90° to the body, due to the low mass of the tail relative to the head region. We estimated that wave-like bending of the body from side to side during steady undulatory swimming moves the COM in the sway (*y*, or side-to-side) direction approximately 5% of the COM excursion amplitude measured in this paper, and has effectively no influence on the COM position in the surge (*x*) or heave (*z*) dimensions. However, as described in more detail below, we quantified the movement of a box-like region surrounding the anatomical COM and this box always contained the actual COM regardless of body posture during swimming.

2.3. Image cross-correlation to measure COM oscillation

We anticipated that COM oscillations during undulatory locomotion would be small and our goal was to interfere with unrestrained fish swimming as little as possible. Therefore, we chose to use image cross-correlation in order to quantify COM motion without attaching transducers with wires to swimming fish and hence possibly altering body motion patterns. One approach would have been to simply digitize the position of a single point near the COM on swimming fishes, but this method is subject to a large error since the COM is not marked, and is time consuming for the number of sequences needed for robust statistical analysis. Instead we used image cross-correlation derived from the technique of particle image velocimetry (PIV) as used in previous research on swimming hydrodynamics (Drucker and Lauder, 1999, 2001; Tytell, 2007; Tytell and Lauder, 2008). We used high-speed video with careful lighting of the swimming fishes to illuminate a patterned area around the COM to obtain a sequence of images of the COM region during swimming, and applied PIV cross-correlation algorithms to calculate the velocity of this region of the body. Instead of tracking particles in the water flow, the PIV cross-correlation algorithms in this case tracked the patterned region of the body. This same image correlation approach has previously been used to study zebrafish locomotion (Danos and Lauder, 2007) and to analyze COM motion during pectoral fin swimming by bluegill sunfish (Lauder and Madden, 2008).

Experiments were conducted in a 60 l flow tank chilled to 16.7 °C for *A. rostrata*, 19 °C for *L. macrochirus* and heated to 24.7 °C for *N. chitala*. Fish were filmed while swimming and holding as steady a position as possible in the water column within a workspace of 20 cm × 19.2 cm × 19 cm at speeds of 0.5, 1.0, and 1.5 BL/s. We made a considerable effort to obtain sequences in which fish were swimming as steadily as possible, but sequences often showed some small drift of the body forward or backward in the flow (in the order of 1–3 mm over several seconds). We corrected for this as described below.

We used two Photron Fastcam high-speed video cameras (1024 × 1024 pixel resolution; Photron, San Diego, CA, USA) recording at 250 fps and synchronized with each other to capture COM motion in three dimensions. The two cameras were placed to capture images from the lateral and ventral views of the swimming fish, with a 45° mirror placed underneath the tank to achieve the ventral view. For *A. rostrata*, the lateral view was not captured as fish swam near the bottom, and instead one camera captured a view of about 16 cm × 16 cm from the ventral view to allow accurate measurement of surge COM motion, while the other camera captured a wider view of 40 cm × 40 cm, also from the ventral view, to allow analysis of sway motion. This wide view additionally allowed quantification of the whole body wave of the swimming eel. These camera positions allowed calculation of COM movement in three dimensions: surge (*x*, or forward/backward, in the streamwise direction), sway (*y*, or side-to-side motion), and heave (*z*, vertical or up/down motion of the COM).

Analysis was conducted by defining either a square or a rectangular region on the body in the digital movie files over the anatomical COM using DaVis software (v 7.2; LaVision Software,

Inc., Goettingen, Germany). This resulted in the creation of a velocity vector field over the area containing the center of mass when analyzed with image cross-correlation between successive video frames. This region was moved with the fish where necessary to ensure that the vector field always included the COM. DaVis software is capable of moving the area of interest with the swimming velocity of the fish so that homologous regions are always sampled. Sample images are shown in Fig. 1 with the collection of vectors representing the velocity of the patterned area over the COM. The supplementary movie in the online Appendix shows vectors over the COM changing with respect to the tail beat in swimming bluegill sunfish as seen in ventral view. This approach has the advantages of (i) making it possible to directly calculate the velocity of the COM region (and avoiding differentiation from displacement data), (ii) resulting in numerous (10–100) velocity vectors from which an average at each time can be calculated, and (iii) generating sub-pixel accuracy estimates of COM motion due to the image correlation approach (see Willert and Gharib, 1991 for details of how cross-correlation results in sub-pixel measurement accuracy). For the ventral view the chosen area was approximately 1 cm × 1 cm for *N. chitala* and *A. rostrata*, and 1.5 cm × 1.5 cm for *L. macrochirus*. The lateral COM area was approximately 2 cm × 2 cm for *L. macrochirus* and *N. chitala* (Fig. 1). Careful playback confirmed that the vectors were, in fact, following the motion of the fish. Custom software was used with Matlab (v 7.1; Mathworks, Inc., Natick, MA, USA) to average the COM velocity vectors exported from DaVis 7.2, giving a single mean velocity vector for each frame in each view, and then a series of mean velocities for the entire swimming sequence. We used this same image correlation procedure to automatically track tail position during the swimming sequences.

2.4. Determining the pattern and magnitude of COM oscillation

To determine the pattern of COM oscillation, if any, the derivative of the velocity trace of each sequence was calculated using Labchart v 7.2 (ADInstruments, Dunedin, New Zealand). This gave the acceleration trace of the COM. Surge direction data was taken from the *x*-component of the calculated velocity vectors in the ventral view, and sway direction data from the *y*-component of the calculated vectors in the ventral view. Ventral view images showed substantially smaller effects of changes in lighting as fish undulated from side to side, and changes in lighting could introduce errors into the *x*-component of COM motion. Heave direction data was taken from the vertical component of vectors in the lateral view (Fig. 1A) and showed minimal effects of changes in lighting. The pattern of COM displacement was determined by integrating the velocity trace (Fig. 1G). A linear regression was then calculated on each segment where the fish was swimming as steadily as possible, and a sum of sines model was fit to the residuals. The maximum number of allowed terms was 3 while maintaining an R^2 of at least 0.80. The crest to trough difference in the plotted curve fit was then calculated to get the overall magnitude of COM excursion (peak-to-peak motion, Fig. 1). This allowed us to detrend sequences in which the fish drifted slightly in the upstream/downstream direction, and we only used sequences in which a significant linear model showed that drift was at constant velocity (i.e., zero acceleration) and that fish were not displaying a mean acceleration during the sequence.

2.5. Validating the COM analysis method

We conducted a series of validation tests to confirm that this image cross-correlation method provided an accurate method for analyzing COM motions by comparing surge and sway displacement values obtained by using image analysis to known displacements. Two possible sources of error in the image correlation method were targeted for testing: (i) the inability of the image correlation analysis to effectively use the fish body pattern to track COM movement, and (ii) errors caused by optical interference from the reflections or compression of scales as the body bends, thus giving a larger velocity than the correct value. The second source of error was potentially an issue only for data derived from the lateral camera view as ventral camera images were not impacted by the side lighting used.

To examine these sources of error, a control system was devised which would output the exact COM displacement of a swimming fish in the surge direction. One specimen of *L. macrochirus* was euthanized gradually with excess tricaine methanesulphonate over the course of 10 min. After complete euthanasia and before the onset of rigor mortis, the fish was attached to a strap directly behind the center of mass using suture and attached to a robotic flapping system typically used in experiments on biomimetic foils (Lauder et al., 2007, 2012; Wen and Lauder, 2013; Quinn et al., 2014). This robotic flapping foil device contains a high-resolution (5 μm accuracy) linear encoder that directly outputs position in the surge direction, and also high-resolution encoders that output side-to-side (sway) displacements. We filmed sequences from both the ventral and lateral view of the dead fish which was moved by the robotic flapper with a sway motion of ±1 cm and at 1 and 2 Hz flapping frequency with free-stream flow that approximated that of fish swimming speeds. Since the fish's COM movement was completely controlled by the flapping apparatus, the encoders attached to the flapping robotic device were able to give the exact position of the fish through time.

Comparison of COM displacement data from the image correlation analysis and the flapping robot encoder data indicated that the error for a dimension on the plane parallel to the camera was about 0.1 mm, which is approximately one order of magnitude lower than our COM oscillation magnitude estimates.

2.6. Amplitude and frequency of the tail beat

The amplitude of the tail beat and fish body shapes during locomotion were estimated using custom Matlab software. Ten midlines of the body and tail during one tail beat cycle were digitized to illustrate the shape of swimming fish (Fig. 2). Tail beat frequency was calculated from the DaVis velocity output with Labchart v 7.2 (ADInstruments). Low-speed swimming sequences for *L. macrochirus* (at 0.5 BL/s) which only involved labriform (pectoral fin) propulsion and little body oscillation were not used for tail beat amplitude calculations.

Two general parameters related to undulatory propulsion were calculated for each sequence: Strouhal number and slip number. These are common metrics used to assess undulatory locomotion (e.g., Gillis, 1997; Triantafyllou et al., 2000). Strouhal number was calculated as $St = (A \times F)/U$, where A is the largest peak-to-peak distance of a tail beat, F is the tail beat frequency, and U is the flume (swimming) speed. Slip number was calculated as $Slip = U/v$, where U is the flume speed and v is the speed of the fish's body wave.

2.7. Statistical analysis

Each species was represented by three specimens except *N. chitala* for which we studied four specimens. Each specimen was filmed twice at three different speeds, giving 56 video sequences containing a combined 123 surge segments, 111 sway segments, and 61 heave segments (with a segment defined as the area over which a linear regression was performed). No heave segments were analyzed for *A. rostrata* as the eels swam near the bottom of the flow tank and we were concerned about bottom effects on COM oscillation patterns. It is possible that anguilliform locomotion involves

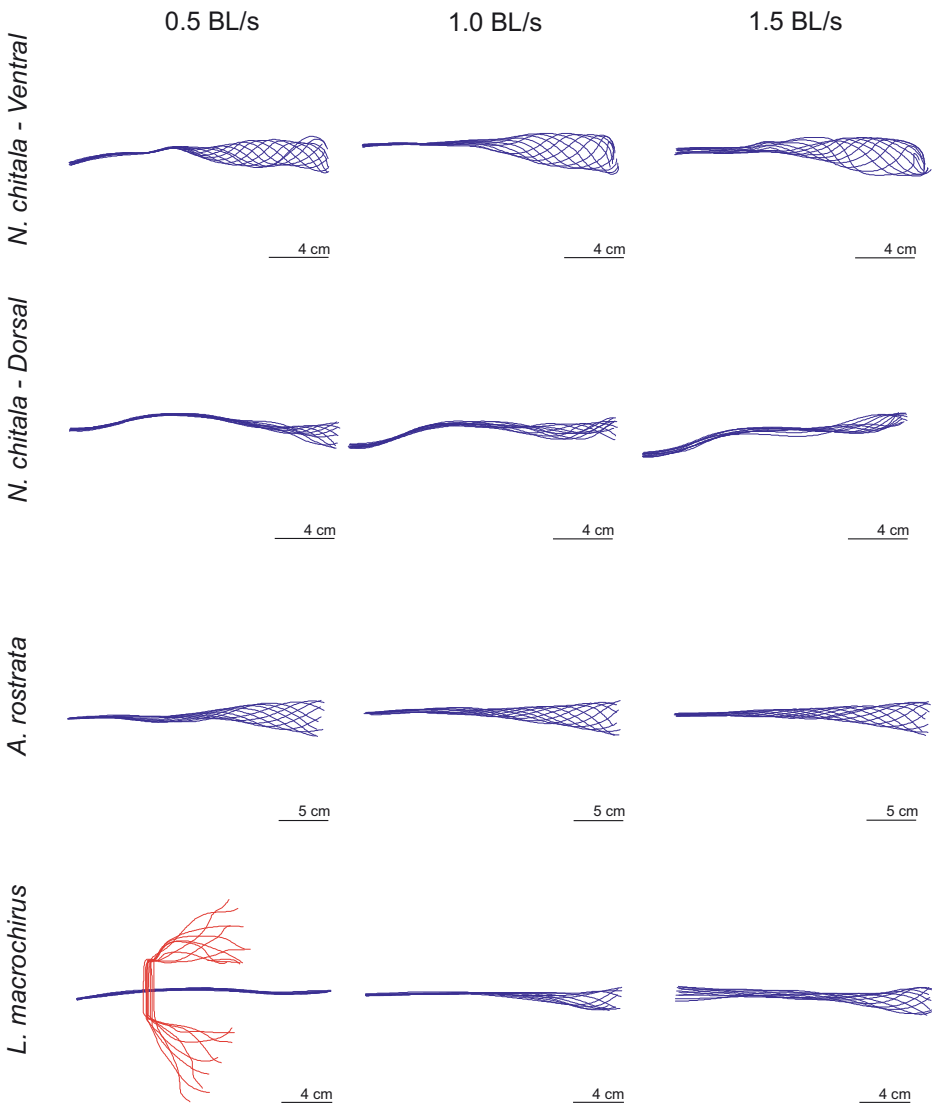

Fig. 2. Representative midlines of swimming fish at three different speeds (blue) and pectoral fin motion for *L. macrochirus* at the slowest swimming speed (red) which show fish movement over one tail beat cycle. Dorsal body curves of *N. chitala* differ from ventral (anal fin) curves in that the amplitude is much smaller and only seen in the posterior quarter of the body. Amplitude of the tail beat did not increase significantly with increasing speed for any of the three species ($p = 0.44$ for *L. macrochirus*, $p = 0.11$ for *A. rostrata*, $p = 0.11$ for *N. chitala*).

small heave oscillations as thrust may not be directed exactly through the COM at all times during swimming, but this condition was not analyzed here. Each analyzed video segment contained between one and five tail beat cycles.

A two-way analysis of variance (ANOVA) was carried out on the surge, sway, and heave COM displacement datasets separately. Where significance was seen, a Tukey HSD post hoc test was carried out at the $p \leq 0.05$ significance level to determine the significance of differences in means among the groups. Significance tests for frequency and amplitude were calculated using a standard least squares linear regression. Data from separate individuals were pooled for this analysis as the data for individuals in the different species and speeds was highly unbalanced and prevented inclusion of a nested level of individuals within species. This analysis used Stata v. 11 (StatCorp, College Station, TX, USA). We conducted separate one-way ANOVA analyses for each species to test for individual effects (using JMP v. 10; SAS Institute, Carey, NC, USA) and found no significant individual effects for the three species studied here.

Species and speed effects for Strouhal and slip number were each calculated using a two-way analysis of variance (ANOVA). These statistical analyses were carried out using Stata v. 11.

3. Results

3.1. General locomotor patterns

As swimming speed increased, the amplitude of the tail beat did not increase significantly for any of the three species ($p = 0.44$ for *L. macrochirus*, $p = 0.11$ for *A. rostrata*, $p = 0.11$ for *N. chitala*; see Fig. 2). Frequency (freq), on the other hand, had a significant positive relationship ($p < 0.001$) with swimming speed for all the species (Fig. 3). The relationship for *L. macrochirus* was freq = 1.67 × speed + 0.51 ($R^2 = 0.88$), for *A. rostrata* freq = 1.43 × speed + 0.19 ($R^2 = 0.83$), and for *N. chitala* freq = 1.63 × speed + 0.54 ($R^2 = 0.94$). There was no significant difference of slope among species (Fig. 3; linear regression $p = 0.77$). At the slowest swimming speed of 0.5 BL/s, *L. macrochirus*

Table 1
Fin beat frequency, Strouhal number, and slip number for the three fish species studied here (bluegill sunfish, *Lepomis macrochirus*; eel, *Anguilla rostrata*; and clown knifefish, *Notopterus chitala*) swimming steadily at three speeds. Strouhal and slip numbers are dimensionless.

Species	Speed (BL/s)	Fin beat frequency (Hz)	Strouhal number	Slip number
L. macrochirus	0.5	1.21 ± 0.08	–	–
L. macrochirus	1	2.24 ± 0.13	0.23 ± 0.02	0.37 ± 0.01
L. macrochirus	1.5	3.22 ± 0.10	0.26 ± 0.01	0.47 ± 0.01
A. rostrata	0.5	0.78 ± 0.04	0.32 ± 0.03	0.88 ± 0.05
A. rostrata	1	1.85 ± 0.12	0.36 ± 0.03	0.66 ± 0.04
A. rostrata	1.5	2.19 ± 0.09	0.28 ± 0.01	0.78 ± 0.04
N. chitala	0.5	1.35 ± 0.05	0.51 ± 0.03	0.58 ± 0.02
N. chitala	1	2.19 ± 0.10	0.36 ± 0.02	0.79 ± 0.02
N. chitala	1.5	2.98 ± 0.08	0.34 ± 0.01	0.85 ± 0.03

Kinematic parameters for each species at 0.5, 1.0, and 1.5 body lengths/s are means ± S.E. Amplitude of the tail beat did not increase significantly with increasing speed for any of the three species. Frequency, on the other hand, had a significant positive relationship ($p < 0.001$) for each species. Strouhal number (based on tail tip amplitude) and slip number were not calculated for *L. macrochirus* at 0.5 BL/s because at this speed there is no body undulation, only pectoral fin (labriform) propulsion.

swam using only the pectoral fins, and for the statistical comparisons pectoral frequency was substituted for tail beat frequency at this speed. As speed increased, sunfish displayed increasing lateral oscillation amplitudes anteriorly. Lateral excursion showed increasing amplitude down the body, and for knifefish the anterior half of the body did not display much lateral oscillation at any speed (Fig. 2). Waveforms differed for the dorsal and ventral views of knifefish because the dorsal view reflects the pattern of body bending, while the ventral view measures motion of the elongate anal fin (Fig. 2). Anal fin and body thus show decoupled frequencies and amplitudes of motion, and the anal fin waveform is of larger amplitude and begins more anteriorly on the body than the body waveform (Fig. 2).

Strouhal number (see Table 1) had a significant species effect ($F = 18.8$), speed effect ($F = 11.4$), and species × speed interaction effect ($F = 8.6$). Strouhal numbers for *Notopterus* swimming at the slowest speed were the highest observed for all species and all speeds. Slip number (see Table 1) also had a significant species effect ($F = 36.4$), speed effect ($F = 4.4$), and species × speed interaction ($F = 13.1$). Bluegill had relatively low slip numbers compared to the other species.

3.2. Patterns of COM oscillation

L. macrochirus and *A. rostrata* have similar patterns of surge COM movement. For every tail beat cycle that occurs, the COM undergoes two cycles of surge (forward/back) COM movement (Figs. 4 and 5). Sway and heave accelerations oscillated at the tail beat frequency for these two species (Figs. 4 and 5). However, in the clown knifefish, surge COM accelerations occurred at the same frequency as the tail beat (Fig. 6) as did the heave and sway COM accelerations.

A fast Fourier transform (FFT) of these data (Fig. 7) shows that COM acceleration displays higher signal power for the double tail beat frequency than it does for the tail beat frequency in bluegill and eels. COM surge displacement, however, shows a slightly lower peak for the double frequency than the single tail beat frequency (Fig. 7A and B). In contrast, in knifefish, both surge COM acceleration and displacement show very much reduced signal power at double the tail beat frequency compared to that present at the tail beat frequency (Fig. 7C).

Plots of the 3D motion of the COM in each species during a single tail beat cycle at 1.5 BL/s show that the COM moves in a loop with an overall figure-eight configuration (Fig. 8).

Statistical analysis of the COM excursion (displacement) data yielded significant differences among species, speeds, and COM displacement directions (Table 2 and Fig. 8). Surge data exhibited significant overall differences for species ($F = 5.23$) but not for speed ($F = 0.24$). Mean COM oscillations in the surge direction at 0.5 BL/s, peak-to-peak, for *L. macrochirus*, *A. rostrata*, and *N. chitala*, were 1.2, 0.9, and 0.5 mm, respectively. Oscillations for each species at 1.0 BL/s were 1.5, 0.8, and 0.8 mm, and this corresponds to a range from 0.2% to 0.7% body length. Surge oscillations at 1.5 BL/s were 1.4, 0.6, and 0.8 mm. A post hoc Tukey's HSD test yielded significant results only for *L. macrochirus* compared with *A. rostrata* ($F = 4.10$) and compared with *N. chitala* ($F = 4.50$): sunfish have higher surge COM oscillations than the other two species (also see Fig. 9A).

Sway oscillations had a significant effect for species, speed, and the species × speed interaction term ($F = 41.8, 7.4, 5.5$, respectively; Table 2). Mean COM oscillations in the sway direction at 0.5 BL/s, peak-to-peak, for *L. macrochirus*, *A. rostrata*, and *N. chitala* were 0.35, 5.77, and 1.06 mm, respectively. Mean oscillations for 1.0 BL/s were 0.89, 4.03 and 2.34 mm, respectively, and at 1.5 BL/s oscillations were 2.99, 4.7, and 3.21 mm, respectively. A post hoc Tukey's HSD test showed significant differences between *L. macrochirus* and

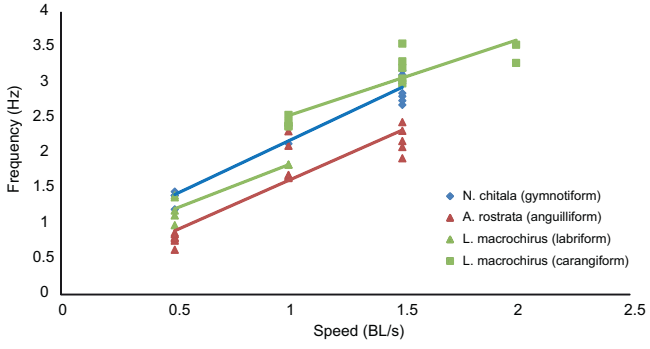

Fig. 3. Speed vs. frequency for three species swimming in four swimming modes. Frequency had a significant positive relationship ($p < 0.001$) for all three species. The relationship for *L. macrochirus* was freq = 1.67 × speed + 0.51 ($R^2 = 0.88$), for *A. rostrata* it was freq = 1.43 × speed + 0.19 ($R^2 = 0.83$), and for *N. chitala* it was freq = 1.63 × speed + 0.54 ($R^2 = 0.94$). There was, however, no significant difference in slope among species ($p = 0.77$). For *L. macrochirus*, pectoral frequency was substituted for tail beat frequency during labriform propulsion at 0.5 BL/s as there was no body undulation at this speed.

Table 2
Two-way ANOVA table to show *F*-values for speed and species effects on each of the three dimensions of center of mass (COM) oscillation.

Direction	Species	Speed (BL/s)	Species × Speed
Surge	5.23 (2, 37)**	0.24 (2, 37)	0.39 (4, 37)
Sway	41.80 (2, 41)***	7.37 (2, 41)***	5.50 (4, 41)***
Heave	0.83 (1, 26)	1.50 (2, 26)*	0.77 (2, 26)

Two-way analysis of variance (ANOVA) was carried out separately for each direction of COM motion (surge, sway, and heave) to assess the speed and species effects. Degrees of freedom for the numerator and denominator are shown in parentheses.
* Significant at $p < 0.05$.
** Significant at $p < 0.01$.
*** Significant at $p < 0.002$.

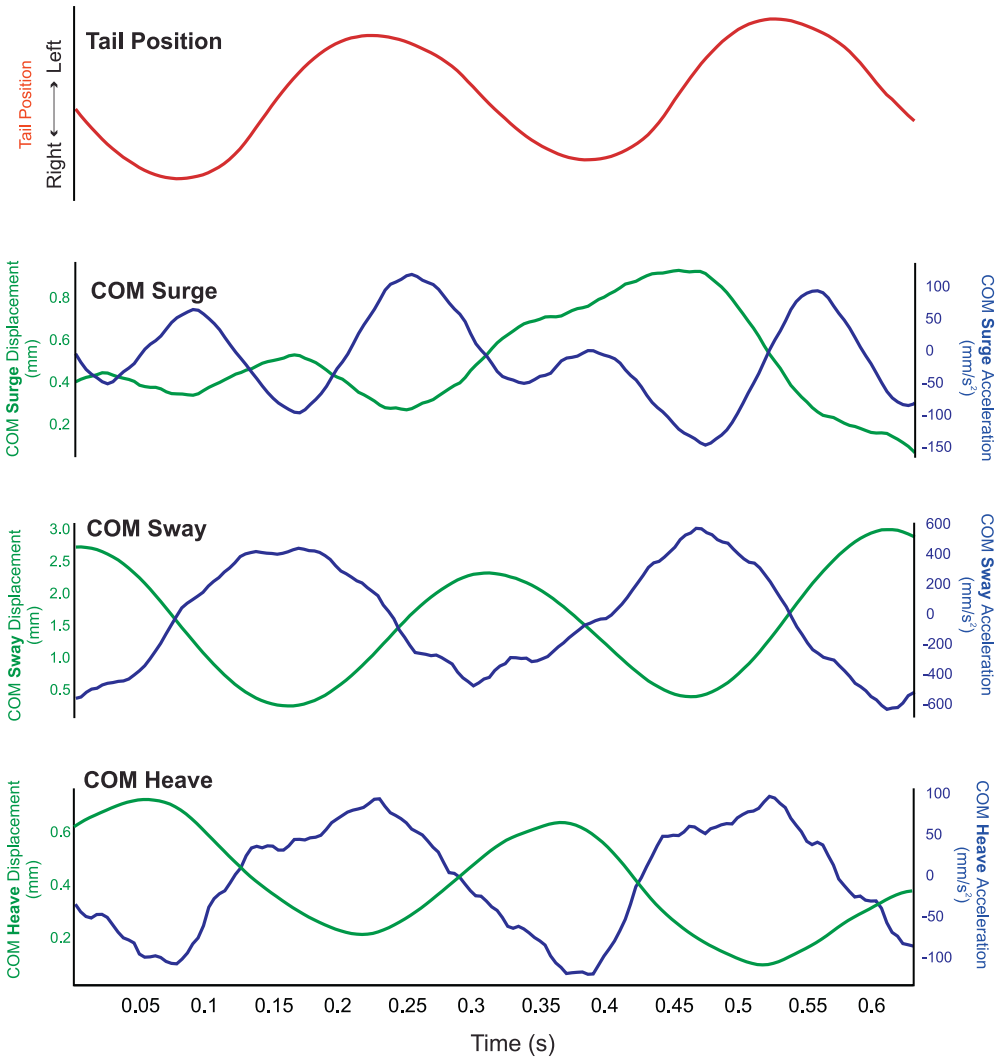

Fig. 4. Center of mass displacement (green curve) and acceleration (blue curve) relative to tail position (red, shown for reference) in *L. macrochirus* swimming at 1.5 BL/s. Surge acceleration shows a double peak oscillation at twice the frequency of the tail beat which is absent in the sway data.

A. rostrata ($F = 13.03$), *L. macrochirus* and *N. chitala* ($F = 3.44$), and *A. rostrata* and *N. chitala* ($F = 9.59$). A post hoc test did not show any significant differences between 0.5 and 1.0 BL/s ($F = 0.37$), but was significant for 0.5 and 1.5 BL/s ($F = 5.07$) and 1.0 and 1.5 BL/s ($F = 5.44$). A one-way ANOVA for all three species showed no significant effect of speed for *A. rostrata* ($F = 2.34$), indicating that the significant speed effect was due to the other two species. Speed effects for *L. macrochirus* and *N. chitala* were not significant between 0.5 and 1.0 BL/s ($F = 0.41$, $F = 0.39$), but were significant for 0.5 and 1.5 BL/s ($F = 5.56$, $F = 5.33$) and 1.0 and 1.5 BL/s ($F = 5.97$, $F = 5.72$). Bluegill and knifefish thus showed increasing sway COM oscillations with speed, but eels did not (Fig. 9B).

Heave COM oscillation was significantly different across speeds ($F = 4.33$) but not across species ($F = 0.83$; no data were taken from *A. rostrata* since eels swam close to the bottom). Mean COM oscillations in the heave direction at 0.5 BL/s were 0.43 and 0.64 mm for *L. macrochirus* and *N. chitala*, respectively. Mean oscillations at 1.0 BL/s were 0.65 and 0.55 mm, respectively, and at 1.5 BL/s oscillations were 0.85 and 1.11 mm, respectively. A post hoc Tukey's HSD test showed significant differences between 1.5 and 0.5 BL/s ($F = 4.25$) and 1.5 and 1.0 BL/s ($F = 3.62$) but not for 0.5 and 1.0 BL/s ($F = 0.64$). Heave COM oscillations thus increased with speed, but the effect was only significant if the lowest and highest swimming speeds are compared in post hoc tests (Fig. 9C).

4. Discussion

In the present paper we present data on fish three-dimensional COM motion with the purpose of (i) providing precise estimates of the magnitude and frequency of COM motion in fishes swimming with undulatory propulsion, and (ii) testing hypotheses about COM oscillation when fishes use four swimming modes over a range of speeds: anguilliform (*A. rostrata*), carangiform and labriform (*L. macrochirus*), and gymnotiform (*N. chitala*). Using an image correlation approach, we tracked the center of mass in three species of fish and used fast Fourier transforms and analyses of COM excursions to describe the pattern of COM oscillation (Figs. 4–6 and 9).

With respect to the four hypotheses outlined at the end of Section 1, we found that (i) anguilliform swimming by eels shows reduced COM surge oscillation magnitude relative to carangiform swimming, but not compared to knifefish using a gymnotiform locomotor style; (ii) labriform swimming (bluegill at 0.5 BL/s) displays reduced COM sway oscillation relative to swimming in a carangiform style at higher speeds; (iii) gymnotiform locomotion displays reduced surge and sway COM oscillation magnitudes compared to some species at some speeds, but not for all comparisons among species and speeds; and (iv) oscillation frequency of the COM in the surge direction occurs at twice the tail beat frequency for carangiform and anguilliform swimming, but not for

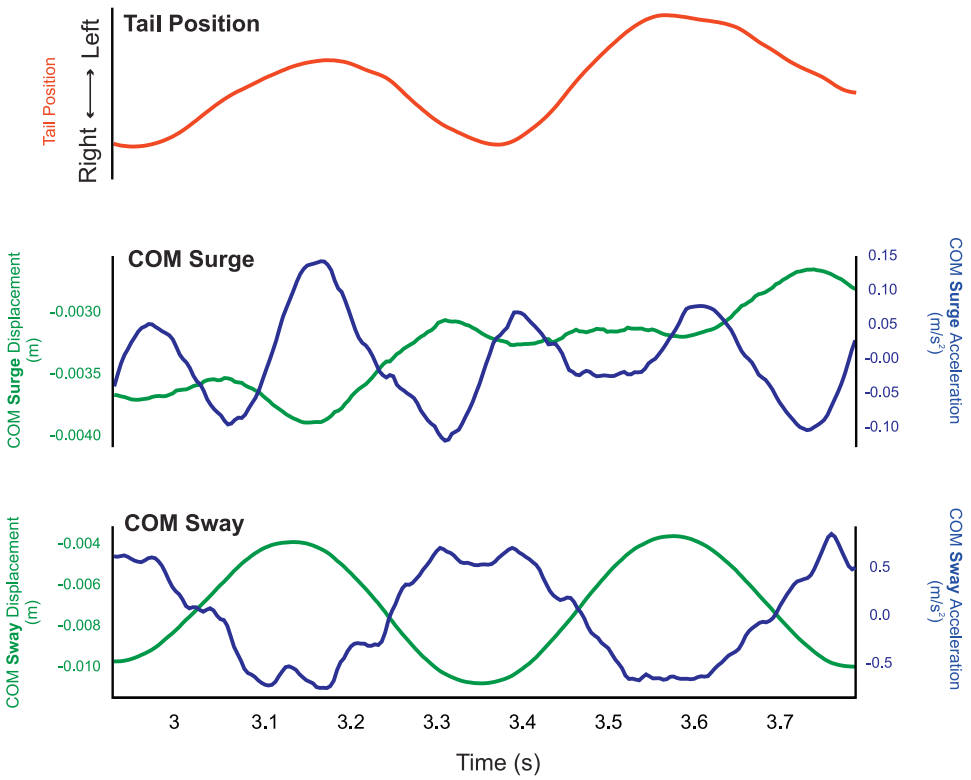

Fig. 5. Center of mass displacement (green curve) and acceleration (blue curve) relative to tail position (red, shown for reference) in *A. rostrata* swimming at 1.5 BL/s. Surge displacement shows a double peak oscillation which is not evident in the sway data. No heave motion was measured in this species as eels swam near the bottom.

gymnotiform locomotion in clown knifefish: knifefish surge COM oscillation occurs most prominently at the *same* frequency as the tail beat.

4.1. COM oscillation and fish swimming modes

The COM of *L. macrochirus* and *A. rostrata* were found to oscillate at twice their tail beat frequency in the surge direction. *N. chitala*, on the other hand, did not show a clear double frequency peak in its COM oscillation, and instead showed a large peak at the tail beat frequency (Fig. 7C) and much less signal power at twice the tail beat frequency. This could be due to the gymnotiform swimming mode with dual waveforms (one from the body, and one from the anal fin), both contributing to thrust. Dual thrust generation mechanisms could smooth out the overall pattern of thrust generation with the effect of greatly reducing the thrust power signature from the tail seen at the COM. In addition, the tail of the clown knifefish is highly tapered with a reduced surface area compared to more anterior regions of the body, and may not generate the large thrust impulses seen in fishes with more generalized symmetrical homocercal tails (Nauen and Lauder, 2002; Tytell, 2007). Classic gymnotiform swimmers like the ghost knifefish *Apteronotus albifrons* have an elongated anal fin attached to a relatively rigid body (Blake, 1983), while *N. chitala* undulates both its trunk and its anal fin with different frequencies and amplitudes (Fig. 2). Without an experimental system in which two such waveforms can be precisely controlled, it will be difficult to test the hypothesis that the dual waveform arrangement in clown knifefish is responsible for the difference in surge COM frequency. Robotic knifefish designs (Shirgaonkar et al., 2008; Curet et al., 2011a,b) or dual biomimetic flapping foils that can generate different wave frequencies and amplitudes may be useful in understanding how knifefish alter COM surge frequencies relative to other fishes. It is noteworthy that knifefish also showed the highest Strouhal numbers (based on the body waveform) at the slow swimming speed (Table 1). This large Strouhal number, generally reflective of relatively inefficient locomotion, may be misleading in not including the propulsive effect of the anal fin.

COM oscillation magnitude for the surge direction was significant only for *L. macrochirus* when compared with either *A. rostrata* or *N. chitala*. This is most likely due to the similar number of waves produced by *A. rostrata* and *N. chitala* – anguilliform and gymnotiform locomotion have at least one wave (crest to crest) present on the body (Lauder, 2006), whereas *L. macrochirus*, using labriform and carangiform motion, has less than one wave on the body during swimming. Slip number, which gives the ratio of swimming speed to body wave speed, was lowest for *L. macrochirus* and higher for *A. rostrata* and *N. chitala*, indicating effective propulsion for its amplitude but not for its wavelength (Table 1). The decrease in number of waves present on the body in bluegill may result in thrust and drag forces generated by body segments producing greater oscillations given that there are fewer numbers of propulsive wave segments on the fish's body active at any one time.

Wen and Lauder (2013) used a mechanical flapping foil apparatus to study the effect of different imposed surge oscillations on the swimming of simple passive flexible foils of similar length and surface area to the fishes studied here. Their apparatus allowed programmed surge oscillations of varying magnitude and phase to be imposed on the swimming foil and they measured the effect of these surge oscillations on locomotor forces and wake flow patterns. They found that surge oscillation magnitudes in the order of 1 mm, when imposed at the correct phase, significantly reduced the oscillation in swimming forces, and suggested that this oscillation mimicked the COM oscillations that would be seen in a freely swimming foil or fish of equivalent area. The surge oscillation magnitudes measured for the swimming foils are thus similar to the surge COM magnitudes for swimming bluegill and eels (Fig. 9) and may reflect the necessary axial oscillation of self-propelled swimming bodies during undulatory locomotion.

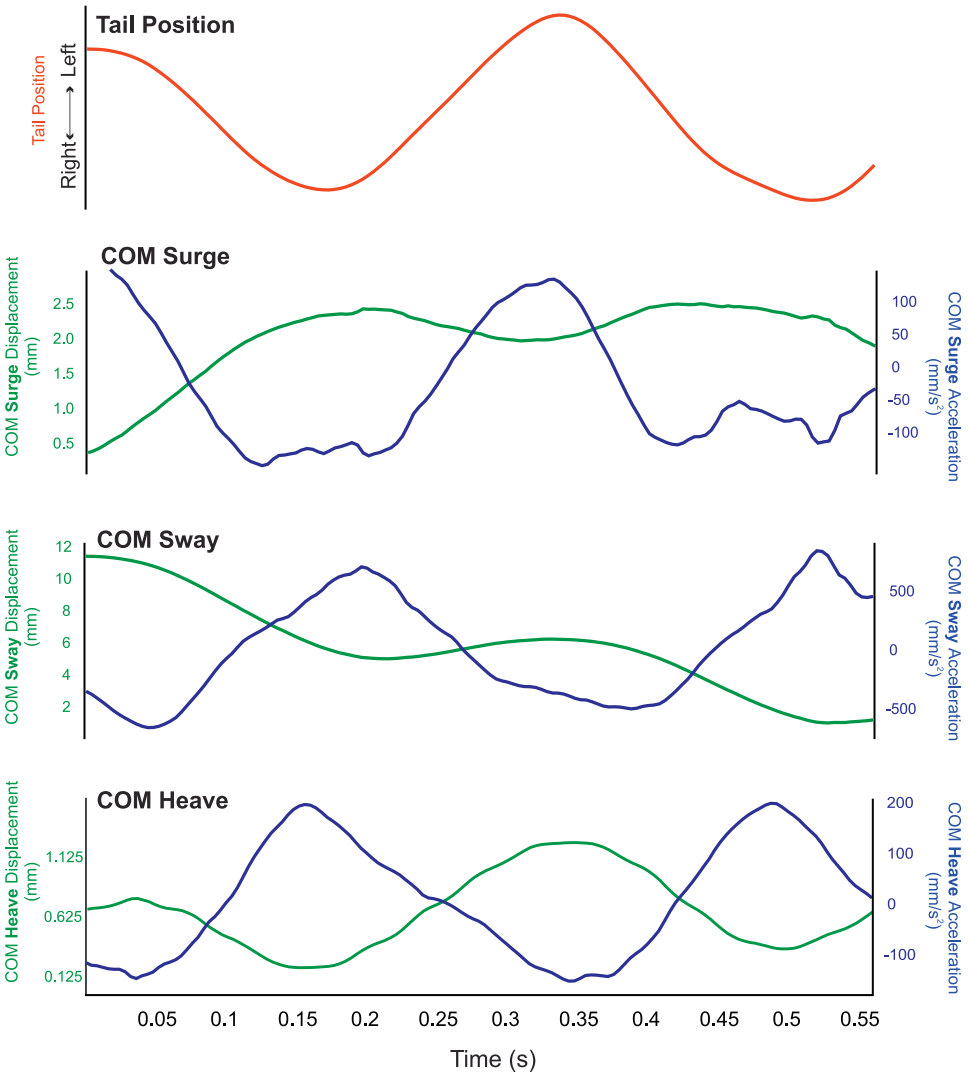

Fig. 6. Center of mass displacement (green curve) and acceleration (blue curve) relative to tail position (red, shown for reference) in *N. chitala* swimming at 1.5 BL/s. Unlike data from *L. macrochirus* or *A. rostrata*, *N. chitala does* not show evidence of surge acceleration at double the tail beat frequency.

Body motion in the sway direction appears to be affected by mediolateral compression, although not as we expected a priori. While *A. rostrata* showed no speed effect, both *L. macrochirus* and *N. chitala* showed greater overall sway oscillation magnitudes as speed increased. *L. macrochirus* and *N. chitala* have a greater surface area to length ratio (5.1 ± 0.45 cm and 3.6 ± 0.02 cm, respectively) than does *A. rostrata* (1.6 ± 0.07 cm). *A. rostrata* did not show a speed effect on sway magnitude but knifefish and bluegill both did, suggesting that their lateral compression does not insulate them from increased sway oscillations as speed increases. An additional factor that may contribute to this result is that at higher speeds the percentage of the body actively engaged in producing thrust may increase, therefore encompassing the center of mass region to a greater degree as anterior myotomal muscles are activated at higher speeds (see, for example, data from swimming bass in Jayne and Lauder, 1995). Decreased lateral stabilization by pectoral or dorsal fins is also another possible explanation, as dorsal and anal fin area may decrease as fish swimming speed increases (Standen and Lauder, 2005).

Heave direction COM oscillation, unlike the surge direction, showed significant increases in amplitude with speed but had no species effect: both species in which heave COM oscillation was measured showed similar increases with speed (Fig. 9C). The increase in heave COM oscillation with speed for both sunfish and knifefish could be a result of (i) inadequate vertical body stabilization by the median or paired fins as swimming speed increases, and/or (ii) increasing instability as higher speed incident flow impacts fin and body surfaces. The dorsal and anal fins of *L. macrochirus* may produce larger counter-rotating torques at higher speeds during steady swimming for body stabilization, but it is possible that this stabilization does not entirely overcome heave COM instability, leading to increased oscillation at higher speeds (Standen and Lauder, 2005, 2007). For *N. chitala*, the asymmetrical tail and posterior body region may also play a role in increased heave motion with speed. In sharks, for example, the asymmetrical tail creates fluid jets with a vertical component, which may account for increased heave motion (Wilga and Lauder, 2002).

4.2. Comparative COM oscillation patterns in animals

Although data on COM oscillation patterns in fish are scarce, previous work by a wide variety of authors (e.g., Blickhan and Full, 1987; Full and Tu, 1991; Farley and Ko, 1997; Griffin et al., 2004; Orendurff et al., 2004; Clemente et al., 2008; Abourachid et al., 2011; Minetti et al., 2011; O'Neill and Schmitt, 2012) on terrestrial locomotion provides a rich source of comparative information,

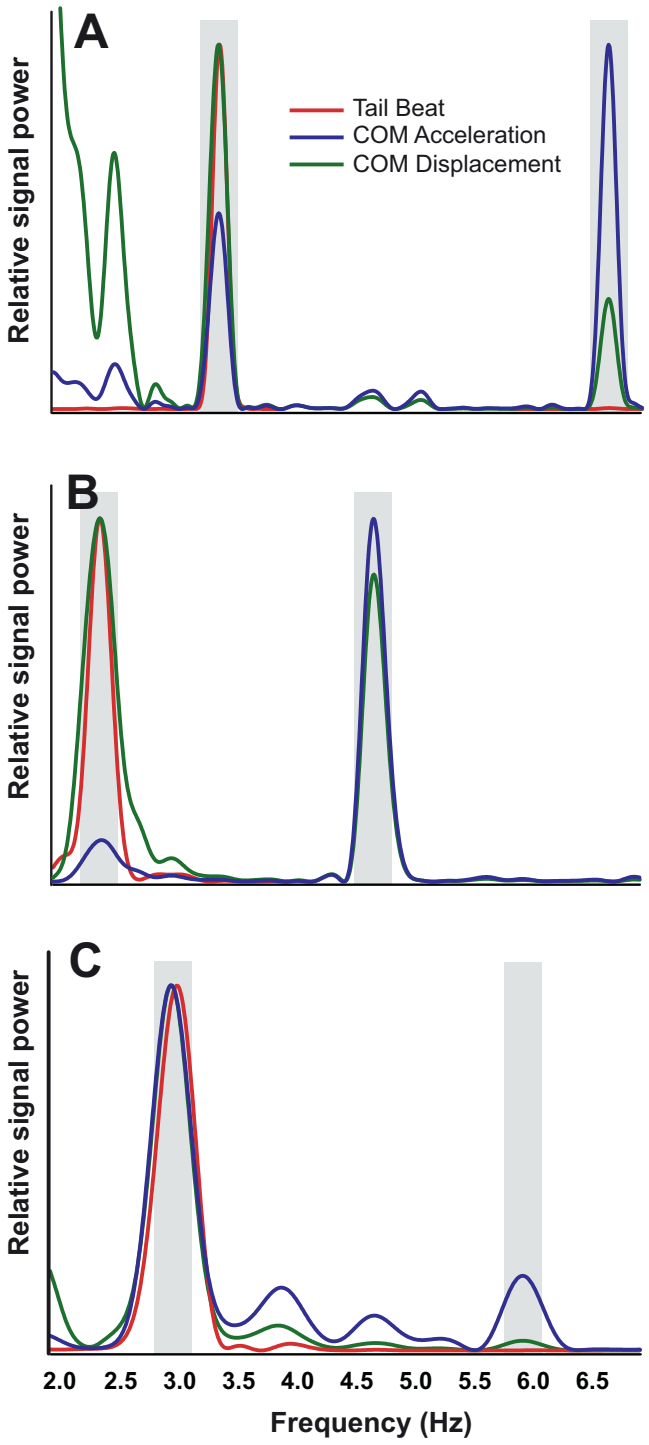

Fig. 7. Fast Fourier transforms of surge COM acceleration and displacement data for locomotion at 1.5 BL/s in (A) *L. macrochirus*, (B) *A. rostrata*, and (C) *N. chitala*. The frequency components of the tail beat are shown for comparison in red. At this speed, *L. macrochirus* uses body and caudal fin undulation and so body undulations are comparable to those of the other species. Grey bars mark the tail beat and double tail beat frequencies. Both *L. macrochirus* and *A. rostrata* show COM acceleration frequency peaks at greater power for double the tail beat frequency than for the single beat frequency, and significant power for displacement at double the tail beat frequency. *N. chitala*, on the other hand, shows minimal power at double the tail beat frequency for acceleration, and negligible power for displacement.

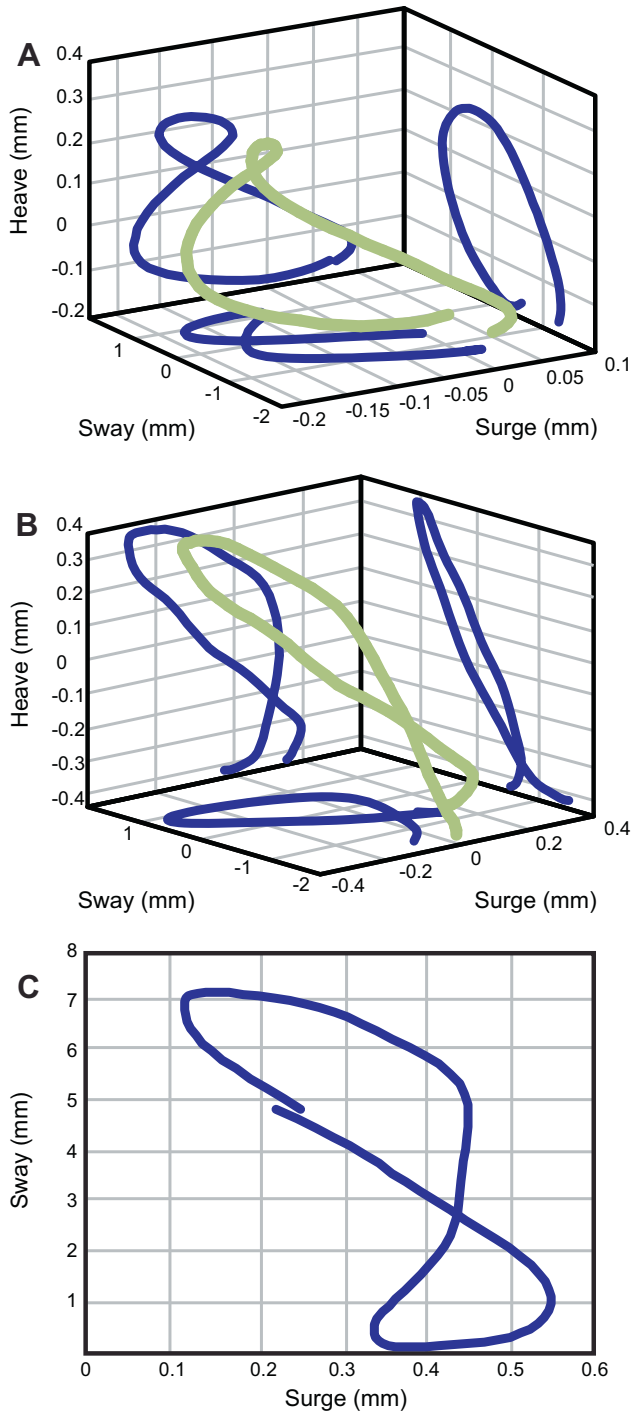

Fig. 8. Center of mass three-dimensional kinematic loop plots for (A) *L. macrochirus*, (B) *N. chitala*, and (C) *A. rostrata* swimming at 1.5 BL/s. 3D loops are shown in green, and the projection seen from each 2D side is shown in blue. We did not measure heave motion for *A. rostrata* as fishes swam near the bottom, and so the figure-8 loop plot shows sway and surge motion only in two dimensions. Loops are not joined exactly at the ends because of small (<0.2 mm) positional drift by the fish body during the tail beat cycle.

and it is instructive to compare COM oscillation amplitudes among the fish species studied here to data from other animals for which COM excursions are available. In studies of terrestrial locomotion, heave COM oscillation amplitudes are the most commonly reported data, and so in Fig. 10 we present an analysis of selected data from the literature showing the scaling relationship between heave COM oscillation (peak-to-peak) excursions and body mass during

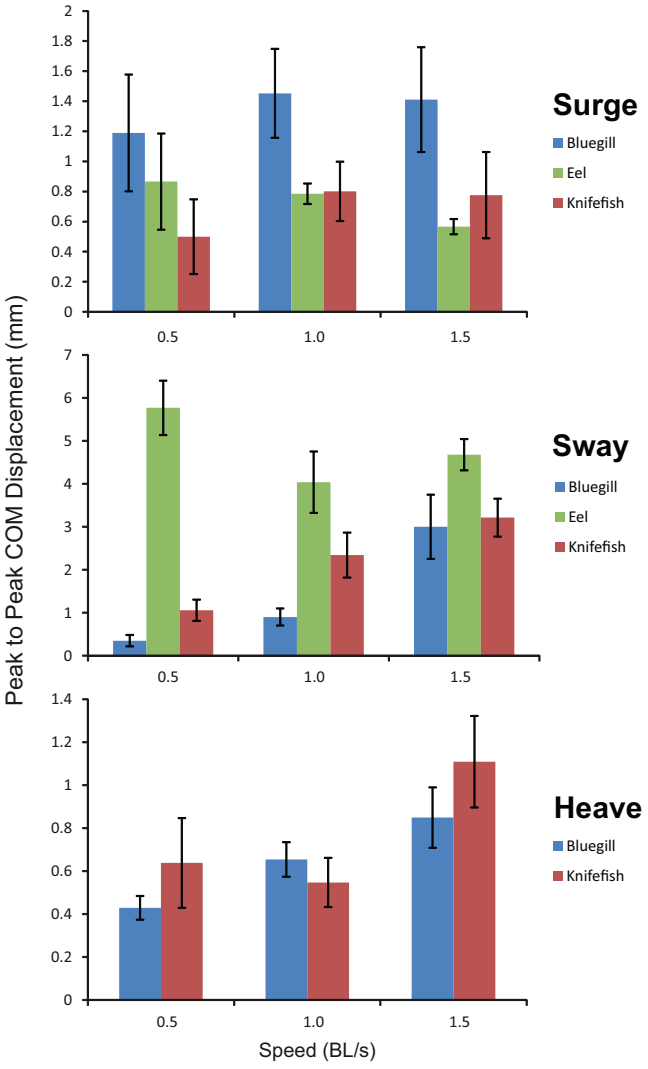

Fig. 9. Center of mass oscillation peak-to-peak magnitudes (i.e., double the wave amplitude) for three dimensions in three species and at three speeds ± 1 S.E. Heave motion was not recorded for *A. rostrata* as this species swam near the bottom. Two-way ANOVA (results given in Table 2) showed a significant species effect for surge; sway data had a significant species, speed, and species × speed interaction effect, while heave data showed a significant speed effect.

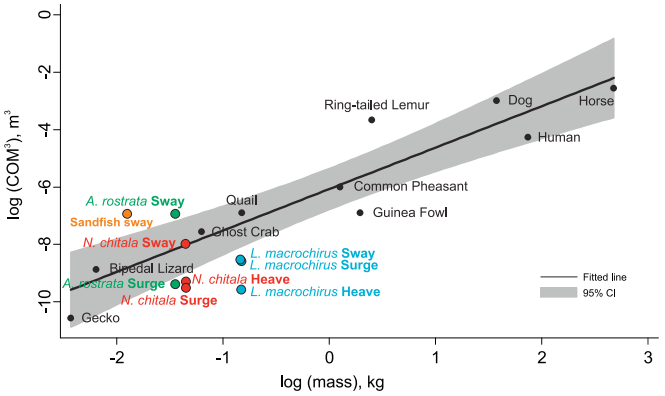

Fig. 10. Comparison of COM oscillation magnitude for different animals. COM oscillation magnitude (peak-to-peak) in each direction was averaged across speeds for terrestrial species to give a single number generally representative of each species. Non-fish data were taken from the literature, and represent COM heave (vertical) motion only since this is the most commonly reported direction of COM oscillation, except for the sandfish point which represents sway motion. Fish data (green, red, and blue points) are from the present study and excursions are shown for all three different measured directions: heave, surge, and sway. The linear fit for data on terrestrial animals shown is $1.44x - 6.07$ ($R^2 = 0.88$), indicating that COM displacement scales positively with mass, and that larger animals display a larger vertical oscillation than would be expected for their size. Fish have significantly lower heave COM oscillations than terrestrial animals. The orange point represents lizard sandfish moving in a granular medium and is derived from Ding et al. (2012).

terrestrial locomotion. Comparison of fish COM oscillations in surge, sway, and heave shows that fish have relatively low heave COM oscillations for their mass (Fig. 10): heave data points for sunfish and knifefish fall well outside the 95% confidence band for the terrestrial heave regression. Heave COM motion of *L. macrochirus* was particularly low, and may be due to the cupped motion of the pectoral fin during propulsion that has been implicated in reducing heave oscillation amplitudes (Lauder and Madden, 2007; Dong et al., 2010). The linear fit of data on terrestrial animals (excluding fish) in Fig. 10 is $6.07 \pm 0.31 + 1.44 \pm 0.19x$ ($R^2 = 0.88$). This slope of 1.44 is significantly greater than the expected isometric slope of 1.0 (length cubed scaled against mass), indicating that COM displacement scales positively with mass, and that larger animals have a larger oscillation than would be expected for their size. The reason for this is unclear at this time, but a simple scaling argument would suggest that since body mass scales to the power of 3 but muscle cross-sectional area scales to the power of 2, the cost of elevating the COM should scale to the 3/2. Although this argument supports the positive scaling seen in the data, many complexities such as elastic energy recovery from muscles and tendons, gait changes, and limb posture changes in animals of different sizes could change how limb muscle force is translated into COM heave (vertical) excursion.

Sandfish lizards (Ding et al., 2012) display higher sway COM oscillations than either knifefish or bluegill, but their COM sway oscillation is similar to that of eels (Fig. 10) even though they are moving through a dense granular medium.

This first analysis of COM scaling involves several limitations as it mixes animals moving with different gaits and speeds (we used the mean COM heave oscillation for all speeds studied for that animal). While this could affect the calculated slope, it seems clear that fish exhibit relatively low heave COM oscillations, in part no doubt due to their undulatory locomotor mode that does not involve pendular or spring-like contacts of limbs with a rigid substrate. Fluid locomotion is generally wave-based and involves thrust and drag forces, while terrestrial locomotion is limb-based and is associated with ground reaction forces (Lighthill, 1971; Farley et al., 1993; Griffin et al., 2004). Wave-based propulsion operates around nodes placed on a line of symmetry down the sagittal plane of the fish, juxtaposing thrust and drag around the COM in the surge direction, although asymmetrical fish body morphology around a horizontal axis could still result in COM heave oscillations. Comparisons across species and modes of locomotion in the future could also shed some light on whether minimizing COM oscillations conserves or requires energy input – a topic subject to much debate in studies on human locomotion (Saunders et al., 1953; Ortega and Farley, 2005; Kuo, 2007).

Although it may seem odd at first glance to compare heave oscillations in fishes to those of terrestrial species, heave oscillations during undulatory propulsion may well represent an energetic cost. Minimizing heave oscillations even during aquatic locomotion may be desirable from an energetic perspective, and not that dissimilar from similar arguments made for terrestrial locomotion. Similarly, sway motions could represent "wasted" energy that reduces locomotor efficiency, and comparisons of sway movement among animals could be informative as part of a broad comparison of locomotor strategies that reduce COM motion in lateral and vertical dimensions. Unfortunately, no simple models of aquatic propulsion similar in form to terrestrial spring mass or inverted

pendulum models are available to make energetic arguments about the significance of different COM motion patterns, and this is an area of future work that may be particularly profitable.

4.3. Future questions for studying fish COM oscillation

Our study provides data on COM oscillation patterns and frequencies in three species of fish that use different undulatory locomotor styles. At this time, wider comparisons with other fish species or over a wider speed range are not possible due to the lack of data in the literature, but a more comprehensive analysis of COM oscillation and its implications for terrestrial and aerial locomotion would be instructive.

We believe that analyses of fish COM motion and the implications of different motion patterns are significantly understudied in comparison to the many studies focusing on other aspects of fish kinematics. There are several key areas where a focus on fish COM oscillation patterns could be instructive.

First, fish locomotor patterns are often described by kinematics that measure body bending, body wavelength and wave number, but the relationship of these more traditional kinematic measurements to movement of the fish COM is unknown. Could it be possible, for example, to define traditional fish kinematic categories such as anguilliform, carangiform, or subcarangiform COM oscillation patterns and to establish correlations between body bending patterns and COM oscillation?

Second, a number of scaling questions emerge from the present study that involve both broader conceptual issues as well as technical issues. How does COM oscillation scale in fish of different sizes? Are the allometric slopes for the three directions of motion in fishes similar to those of terrestrial species, and do the intercepts vary among motion in the aquatic, terrestrial, and aerial locomotor environments? An allied question is to investigate how best to analyze COM oscillations. Is mass the best independent variable in aquatic systems where fluid added mass effects and substantially different projected body surface areas in the three planes of motion could alter expected scaling relationships?

Third, what are the energetic implications of different COM oscillation patterns? In the present paper we have focused on movement patterns of the COM, but the effect of COM oscillation on swimming energetics is unknown. We are not aware of any studies that measure energetics and COM motion together in fishes. And for aquatic undulatory locomotion there is no model (such as a spring mass or inverted pendulum) comparable to these well-established models for terrestrial locomotion that could be used to make an energetic argument.

Fourth, COM acceleration provides an estimate of locomotor forces that act on the individual fish (Walker, 2004), and the data provided here can be used to estimate these forces given the known fish masses. Such force estimates for undulating bodies are not without challenges, however, as including a time-varying added mass component which must be estimated and the effects of friction and pressure drag during undulation are non-trivial issues. It would be instructive in the future to compare locomotor forces estimated from COM motion to those estimated from PIV calculations of wake flow patterns (Drucker and Lauder, 1999; Peng et al., 2007).

Fifth, from a technical perspective, COM analyses could be improved by the incorporation of lightweight accelerometers (suitable for implantation into fishes) along the lines of the technique used in the study of Pfau et al. (2006) on horses. Direct transduction of body accelerations would facilitate the acquisition of greater sample sizes and the comparative study of COM motion, as long as the relatively subtle motions of the COM are not influenced by transducer wires and their implantation.

Finally, given the increasing prominence of robotic models for aquatic propulsion and the development of autonomous fish-like devices, we believe that the use of COM oscillation amplitudes in the surge, sway, and heave dimensions as a performance metric for the comparison of robotic devices with freely swimming fishes holds considerable promise. Autonomous robotic models with COM displacement oscillations in the order of 0.2–0.7% body length will likely perform well, and COM oscillations could be used as a quantitative metric for comparison among different designs and actuation programs. Robotic swimming systems with large COM oscillations will likely incur a high cost of transport and be relatively inefficient.

Acknowledgements

Special thanks to Ryan Shelton and Chuck Witt for their help with Matlab programming, and to Jeanette Lim, Ryan Shelton, Chuck Witt, and Li Wen for insightful discussions. Eric Tytell and Anabela Maia also provided helpful comments on this work and discussions on fish COM oscillations. Dan Goldman and his laboratory kindly suggested comparisons with sandfish COM motions, and Dan Lieberman and Andy Biewener provided useful comments on the terrestrial COM scaling relationship. Thanks also to two anonymous reviewers for their helpful comments, and to Jeff Walker for his thoughts on studying COM motion in swimming fishes and comments on a previous version of this paper. Funding was provided by the Office of Naval Research (grant N00014-09-1-0352 monitored by Dr. Thomas McKenna), and the National Science Foundation (grants EFRI-0938043 and CDI 0941674).

Appendix A. Supplementary data

Supplementary data associated with this article can be found, in the online version, at http://dx.doi.org/10.1016/j.zool.2014.03.002.

References

Abourachid, A., Hackert, R., Herbin, M., Libourel, P.A., Lambert, F., Gioanni, H., Provini, P., Blazevic, P., Hugel, V., 2011. Bird terrestrial locomotion as revealed by 3D kinematics. Zoology 114, 360–368.

Biewener, A.A., 1989. Scaling body support in mammals – limb posture and muscle mechanics. Science 245, 45–48.

Biknevicius, A.R., Reilly, S.M., McElroy, E.J., Bennett, M.B., 2013. Symmetrical gaits and center of mass mechanics in small-bodied, primitive mammals. Zoology 116, 67–74.

Blake, R.W., 1983. Swimming in the electric eels and knifefishes. Can. J. Zool. 61, 1432–1441.

Blickhan, R., Full, R.J., 1987. Locomotion energetics of the ghost crab. 2. Mechanics of the center of mass during walking and running. J. Exp. Biol. 130, 155–174.

Clemente, C.J., Withers, P.C., Thompson, G., Lloyd, D., 2008. Why go bipedal? Locomotion and morphology in Australian agamid lizards. J. Exp. Biol. 211, 2058–2065.

Curet, O.M., Patankar, N.A., Lauder, G.V., MacIver, M.A., 2011a. Aquatic manoeuvering with counter-propagating waves: a novel locomotive strategy. J. R. Soc. Interface 8, 1041–1050.

Curet, O.M., Patankar, N.A., Lauder, G.V., MacIver, M.A., 2011b. Mechanical properties of a bio-inspired robotic knifefish with an undulatory propulsor. Bioinspir. Biomim. 6, 026004.

Danos, N., Lauder, G.V., 2007. The ontogeny of fin function during routine turns in zebrafish (*Danio rerio*). J. Exp. Biol. 210, 3374–3386.

Ding, Y., Sharpe, S.S., Masse, A., Goldman, D.I., 2012. Mechanics of undulatory swimming in a frictional fluid. PLoS Comput. Biol. 8, e1002810.

Dong, H., Bozkurttas, M., Mittal, R., Madden, P., Lauder, G.V., 2010. Computational modeling and analysis of the hydrodynamics of a highly deformable fish pectoral fin. J. Fluid Mech. 645, 345–373.

Drucker, E.G., Lauder, G.V., 1999. Locomotor forces on a swimming fish: three-dimensional vortex wake dynamics quantified using digital particle image velocimetry. J. Exp. Biol. 202, 2393–2412.

Drucker, E.G., Lauder, G.V., 2001. Wake dynamics and fluid forces of turning maneuvers in sunfish. J. Exp. Biol. 204, 431–442.

Farley, C.T., Ko, T.C., 1997. Mechanics of locomotion in lizards. J. Exp. Biol. 200, 2177–2188.

Farley, C.T., Glasheen, J., McMahon, T.A., 1993. Running springs – speed and animal size. J. Exp. Biol. 185, 71–86.

Full, R.J., Tu, M.S., 1991. Mechanics of a rapid running insect: 2-legged, 4-legged, and 6-legged locomotion. J. Exp. Biol. 156, 215–231.

Gibb, A., Jayne, B.C., Lauder, G.V., 1994. Kinematics of pectoral fin locomotion in the bluegill sunfish *Lepomis macrochirus*. J. Exp. Biol. 189, 133–161.

Gillis, G.B., 1997. Anguilliform locomotion in an elongate salamander (*Siren intermedia*): effects of speed on axial undulatory movements. J. Exp. Biol. 200, 767–784.
Griffin, T.M., Main, R.P., Farley, C.T., 2004. Biomechanics of quadrupedal walking: how do four-legged animals achieve inverted pendulum-like movements? J. Exp. Biol. 207, 3545–3558.
Jayne, B.C., Lauder, G.V., 1995. Red muscle motor patterns during steady swimming in largemouth bass: effects of speed and correlations with axial kinematics. J. Exp. Biol. 198, 1575–1587.
Kuo, A.D., 2007. The six determinants of gait and the inverted pendulum analogy: a dynamic walking perspective. Hum. Movement Sci. 26, 617–656.
Lauder, G.V., 2006. Locomotion. In: Evans, D.H., Claiborne, J.B. (Eds.), The Physiology of Fishes. CRC Press, Boca Raton, pp. 3–46.
Lauder, G.V., Madden, P.G.A., 2007. Fish locomotion: kinematics and hydrodynamics of flexible foil-like fins. Exp. Fluids 43, 641–653.
Lauder, G.V., Madden, P.G.A., 2008. Advances in comparative physiology from high-speed imaging of animal and fluid motion. Annu. Rev. Physiol. 70, 143–163.
Lauder, G.V., Anderson, E.J., Tangorra, J., Madden, P.G.A., 2007. Fish biorobotics: kinematics and hydrodynamics of self-propulsion. J. Exp. Biol. 210, 2767–2780.
Lauder, G.V., Flammang, B.E., Alben, S., 2012. Passive robotic models of propulsion by the bodies and caudal fins of fish. Integr. Comp. Biol. 52, 576–587.
Lighthill, M.J., 1971. Large-amplitude elongated-body theory of fish locomotion. Proc. R. Soc. Lond. B 179, 125–138.
Minetti, A.E., Cisotti, C., Mian, O.S., 2011. The mathematical description of the body centre of mass 3D path in human and animal locomotion. J. Biomech. 44, 1471–1477.
Nauen, J.C., Lauder, G.V., 2002. Hydrodynamics of caudal fin locomotion by chub mackerel, *Scomber japonicus* (Scombridae). J. Exp. Biol. 205, 1709–1724.
O'Neill, M.C., Schmitt, D., 2012. The gaits of primates: center of mass mechanics in walking, cantering and galloping ring-tailed lemurs, *Lemur catta*. J. Exp. Biol. 215, 1728–1739.
Orendurff, M.S., Segal, A.D., Klute, G.K., Berge, J.S., Rohr, E.S., Kadel, N.J., 2004. The effect of walking speed on center of mass displacement. J. Rehabil. Res. Dev. 41, 829–834.
Ortega, J.D., Farley, C.T., 2005. Minimizing center of mass vertical movement increases metabolic cost in walking. J. Appl. Physiol. 99, 2099–2107.
Peng, J., Dabiri, J.O., Madden, P.G., Lauder, G.V., 2007. Non-invasive measurement of instantaneous forces during aquatic locomotion: a case study of the bluegill sunfish pectoral fin. J. Exp. Biol. 210, 685–698.
Pfau, T., Witte, T.H., Wilson, A.M., 2006. Centre of mass movement and mechanical energy fluctuation during gallop locomotion in the thoroughbred racehorse. J. Exp. Biol. 209, 3742–3757.
Quinn, D.B., Lauder, G.V., Smits, A.J., 2014. Scaling the propulsive performance of heaving flexible panels. J. Fluid Mech. 738, 250–267.
Saunders, J.B.D.M., Inman, V.T., Eberhart, H.D., 1953. The major determinants in normal and pathological gait. J. Bone Joint Surg. 35A, 543–558.
Sfakiotakis, M., Lane, D.M., Davies, J.B.C., 1999. Review of fish swimming modes for aquatic locomotion. IEEE J. Ocean. Eng. 24, 237–252.
Shadwick, R.E., Lauder, G.V., 2006. Fish Biomechanics. Academic Press, San Diego.
Shirgaonkar, A.A., Curet, O.M., Patankar, N.A., MacIver, M.A., 2008. The hydrodynamics of ribbon-fin propulsion during impulsive motion. J. Exp. Biol. 211, 3490–3503.
Standen, E.M., Lauder, G.V., 2005. Dorsal and anal fin function in bluegill sunfish *Lepomis macrochirus*: three-dimensional kinematics during propulsion and maneuvering. J. Exp. Biol. 208, 2753–2763.
Standen, E.M., Lauder, G.V., 2007. Hydrodynamic function of dorsal and anal fins in brook trout (*Salvelinus fontinalis*). J. Exp. Biol. 210, 325–339.
Triantafyllou, M.S., Triantafyllou, G.S., Yue, D.K.P., 2000. Hydrodynamics of fishlike swimming. Annu. Rev. Fluid Mech. 32, 33–53.
Tytell, E.D., 2007. Do trout swim better than eels? Challenges for estimating performance based on the wake of self-propelled bodies. Exp. Fluids 43, 701–712.
Tytell, E.D., Lauder, G.V., 2008. Hydrodynamics of the escape response in bluegill sunfish, *Lepomis macrochirus*. J. Exp. Biol. 211, 3359–3369.
Walker, J.A., 2004. Dynamics of pectoral fin rowing in a fish with an extreme rowing stroke: the threespine stickleback (*Gasterosteus aculeatus*). J. Exp. Biol. 207, 1925–1939.
Walker, J.A., Westneat, M.W., 1997. Labriform propulsion in fishes: kinematics of flapping aquatic flight in the bird wrasse *Gomphosus varius* (Labridae). J. Exp. Biol. 200, 1549–1569.
Walter, R.M., Carrier, D.R., 2011. Effects of fore-aft body mass distribution on acceleration in dogs. J. Exp. Biol. 214, 1763–1772.
Webb, P.W., 1975. Hydrodynamics and energetics of fish propulsion. Bull. Fish. Res. Board Can. 190, 1–158.
Wen, L., Lauder, G.V., 2013. Understanding undulatory locomotion in fishes using an inertia-compensated flapping foil robotic device. Bioinspir. Biomim. 8, 046013.
Wilga, C.D., Lauder, G.V., 2002. Function of the heterocercal tail in sharks: quantitative wake dynamics during steady horizontal swimming and vertical maneuvering. J. Exp. Biol. 205, 2365–2374.
Willert, C.E., Gharib, M., 1991. Digital particle image velocimetry. Exp. Fluids 10, 181–193.